Soft Matter

Accepted Manuscript

This article can be cited before page numbers have been issued, to do this please use: L. N. Jimenez, C. D. V. Martínez Narváez, C. Xu, S. Bacchi and V. Sharma, *Soft Matter*, 2021, DOI: 10.1039/D0SM02248A.

ROYAL SOCIETY OF CHEMISTRY

rsc.li/soft-matter-journal

View Article Online
DOI: 10.1039/D0SM02248A

The Rheologically-Complex Fluid Beauty of Nail Lacquer Formulations

Leidy Nallely Jimenez, Carina D. V. Martínez Narváez, Chenxian Xu, Samantha Bacchi, and Vivek Sharma*, Department of Chemical Engineering, University of Illinois at Chicago, IL, 60608, USA.

*Correspondence to: Vivek Sharma (E-mail: viveks@uic.edu)

Abstract

Nail lacquer formulations are multi-ingredient complex fluids with additives that affect color, smell, texture, evaporation rate, viscosity, stability, leveling behavior, consumer's sensory experience, and dried coating's decorative and wear performance. Optimizing and characterizing the formulation rheology is critical for achieving longer shelf-life, better control over the nail painting process and adhesion, continuous manufacturing of large product volumes, and increasing overall consumer satisfaction. Dispensing, bottle filling, brush application, and dripping, as well as perceived tackiness of nail polishes, all involve capillarity-driven pinching flows associated with strong extensional deformation fields. However, a significant lack of characterization of pinching dynamics and extensional rheology response of multicomponent formulations, especially particle suspensions in viscoelastic solutions, motivates this study. Here, we characterize the shear rheology response of twelve commercial nail lacquer formulations using torsional rheometry and characterize pinching dynamics and extensional rheology response using dripping-onto-substrate (DoS) rheometry protocols we developed. We visualize and analyze brush loading, nail coating, dripping from brush, sagging, and lacquer application on a nail to outline the challenges posed by free-surface flows and non-Newtonian rheology. We find that the radius evolution over time obtained using DoS rheometry displays power law exponents distinct from those exhibited in shear thinning. Both shear and extensional viscosity decrease with deformation rate. However, the extensional viscosity appears to be rate-independent at the highest rates and displays nearly an order of magnitude larger values than the high shear rate viscosity. We envision that the findings and protocols described here will help and motivate industrial scientists to design better multicomponent formulations through a better characterization and understanding of the influence of ingredients like particles and polymers on rheology, processing, and applications.

View Article Online
DOI: 10.1039/D0SM02248A

INTRODUCTION

Nail lacquer, also known as nail polish, varnish, enamel, or nail paint, is a multicomponent formulation designed for painting or coating fingernails and toenails that dries, forming a firmly adhering film that decorates and protects the underlying nail.[1-3] Nail lacquers are classified into different categories based on solvent choice (aqueous or non-aqueous), the film-forming method (drying or photo-polymerization), and ingredient choices that affect color, smell, texture, evaporation rate, viscosity, stability, and sagging behavior.[1-4] Even though alternatives including aqueous and UV-curable formulations are gaining popularity, the most widely used nail lacquers are formulated with colorants and clay particles added to a solution of a film-forming polymer (like nitrocellulose) in a volatile, organic solvent.[1-4] The preference and popularity of nail lacquer, and colored coatings in general, depend on the consumer perception of liquid coating (homogeneity, thickness, and smoothness), the ease of application, drying time, and both decorative (color, gloss, shine, shimmer, or texture) and wear properties of the dried coatings.[1-15] Even though modern formulations are engineered to satisfy these consumer preferences, control over rheology also influences shelf-life and facilitates selecting appropriate mixing and processing protocols for industrial-scale manufacturing.[11-21] However, after surveying the published literature, we found remarkably few shear rheology measurements of nail lacquer formulations and no extensional rheology studies,[1] motivating this study. Here we focus on conceptual and experimental challenges underlying the rheological characterization of twelve nitrocellulose-based commercial nail lacquer formulations and the fluid mechanics and rheology quests relevant to the problem of painting nails or getting them painted. A quote from Picasso echoes our motivations: “I have a horror of people who speak about the beautiful. What is the beautiful? One must speak of problems in painting!”

View Article Online
DOI: 10.1039/D0SM02248A

It is well-established that shear viscosity with a suitable rate-dependent profile enables better control over the shelf-life, pouring and spreading, sagging and leveling, and thickness and homogeneity of coatings,[11-13, 15-18] and to some extent, influence the perception of formulations as 'thick,' 'thin,' 'runny,' 'gloopy, 'gloppy', or 'goopy.' [6, 7, 9-18] Often, the time taken by a liquid neck to pinch-off on dripping from a brush, or on stretching a liquid bridge between a finger and a thumb informs and determines the consumer experience, satisfaction, and perception of heuristic properties like tackiness, stickiness, stringiness, sprayability, or 'gloopiness'.[14, 21-26] In the food, cosmetic and pharmaceutical industry, consumer panels and shear rheology data, complemented with force-distance plots obtained using texture analyzer, are often used for accessing these heuristic properties of formulations.[6, 7, 14, 15, 21-31] Strong extensional kinematics associated with streamwise gradients in the velocity field often arise in pinching necks during drop formation, near curved interfaces during coating flows, and in liquid bridge or filament stretching experiments.[14-21, 26, 27, 32, 33] Thus, correlating the ingredient-sensitive consumer perception of stickiness or stringiness, pinching dynamics, the evolution of viscoelastic interfacial instabilities, and processability to measurable material properties requires the characterization of extensional rheology. However, several practical challenges exist, including sensitivity to deformation history, elastic or inertial flow instabilities, and a limited range of accessible strain or strain rates, in addition to the need for bespoke instrumentation.[19-21, 26, 33-36] Several recent studies describe the use and application of dripping-onto-substrate (DoS) rheometry protocols we developed[36-42] to address many longstanding challenges for characterizing the extensional rheology and pinching dynamics of polymer and polyelectrolytes solutions,[36-41, 43-48] printing inks,[39, 49] micellar solutions,[39, 50-52] food materials (cellulose gum solutions, ketchup, mayo), and cosmetics (hand-cream, and conditioners).[36-41, 43-53] In this contribution, we characterize the extensional rheology response of the nail lacquer formulations using dripping-onto-substrate

View Article Online
DOI: 10.1039/D0SM02248A

(DoS) rheometry protocols by analyzing the neck pinching dynamics of a stretched liquid bridge formed by dripping a finite liquid volume from a nozzle onto a partial-wetting substrate.[36-43]

The nail lacquer market is over ten billion U. S. dollars and growing.[3, 54] The word lacquer originated from the Sanskrit word "*laksha*" or the Hindi "*lakha,*" which refers to the lac insects and the scarlet resin they produce. Due to the enormous number of insects (and maybe the product's value), *lakh* is the Hindi word for a hundred thousand. Ancient texts, including the epic *Mahabharata* by Ved Vyas and Kalidasa's play *Abhigyanshakuntalam,* mention *laksha* or *lakha,* implying its history of use begins in ancient India (1500-500 BCE).[55] The recent advances in methods used for identifying colorants and binders in icons, paintings, and fabrics attest to the use of lac-based dyes and pigments in both Asia and Europe,[56-58] even though texts from the Mediterranean region as early as the 3rd century A.D. mention "λακχα" (*lakcha, lac*), a water-soluble dye imported from the Indian subcontinent. The recipe of water-insoluble lac lake pigments, formed by precipitating lac on alum, is mentioned as early as the 9th century and contains plant-based gums as binders.[56-60] The complex fluids and processes used for painting nails share many attributes with those used for painting walls and canvasses,[8, 9, 11, 13] and the use and choice of pigments, rheology modifiers, film formers, and binders have a 30,000-year tradition and history.[61-65] Nitrocellulose was one of the first polymers to be used commercially[66, 67], including photographic films for making motion pictures[67, 68] "mother-in-law" artificial silks, and as an additive for applications as varied as explosives[69] and car paints in the 1920s. Unlike canvas, cement, or stone, the substrate for applying nail paints (human nail) is a hard and insoluble structural protein (scleroprotein) made up of keratin.[3, 54] Even though the wettability and roughness, as well as diseases and defects of nails too, influence the perceived properties of nail lacquers,[3, 9, 54] here, we restrict attention to the characterization of rheology and pinching

View Article Online
DOI: 10.1039/D0SM02248A

dynamics, being mindful of the challenges posed by unknown and varied compositions of the commercial formulations.

In this contribution, we first describe the shear rheology response obtained using torsional rheometry and experiments used for visualizing brush loading, sagging, and brush application to nails. We confirm that the nail paints are rheologically-complex fluids that display shear thinning and thixotropic behavior or show rate-dependent viscosity response sensitive to the prior deformation history. Next, we employ DoS rheometry protocols to characterize the pinching dynamics and extensional rheology response of the nail lacquer formulations. The local balance of capillarity, inertia and viscous stresses determine the pinching dynamics for Newtonian fluids,[70-72] and additional contributions from rate-dependent viscosity and elastic stresses determine the pinching dynamics for many complex fluids.[26, 36, 39, 72] For Newtonian and power law fluids, the radius evolution of pinching necks can be often fit by $R(t) \propto R_0 X[(t_f - t)/t_{xc}]^{n_e}$ yielding an exponent, n_e, a filament lifespan, t_f, a characteristic time, t_{xc} and a pre-factor, X that are dependent on material properties. Newtonian fluids display $n_e = 2/3$ and $n_e = 1$ for low and high viscosity, respectively, whereas the Generalized Newtonian fluid models[73-75] predict n_e values matched with the power law exponent, n that captures the shear thinning response.[36, 39, 76, 77] In contrast, solutions of high molecular weight polymers often display an elastocapillary response[15, 26, 33, 35-37, 40-49] with an exponential decrease in radius with the decay constant termed as an extensional relaxation time, λ_E. Radius evolution data allows computation of the strain, ε, and the strain-rate, $\dot{\varepsilon}$ dependent extensional viscosity, $\eta_E = \eta_E(\dot{\varepsilon}, \varepsilon, t)$. Polymer solutions display strain hardening behavior even if shear viscosity exhibits shear thinning.[16-21, 26, 33-43] We find that nail lacquer formulations display extensional thinning and show distinct pinching dynamics even if the shear rheology response is comparable. We anticipate that our protocols and findings will

View Article Online
DOI: 10.1039/D0SM02248A

inspire characterization of pinching dynamics and extensional rheology of industrial complex fluids, drive fundamental research on the rheology of particle suspensions formulated in viscoelastic fluids (similar to nail lacquers) and eventually facilitate the macromolecular engineering of formulations.

MATERIALS AND METHODS

Ingredients of the Twelve Nail Polishes

Figure 1. Nail polishes with different brands and colors. (a) OPI Infinite Shine 2 long-lasting nail polishes. From left to right, the colors are Big Apple Red, Nessie Plays Hide & Sea-k, Closer Than You Might Belém, and Getting Nadi On My Honeymoon. (b) CND Vinylux long-wear nail polishes. The colors are Bloodline, Midnight Swim, Lobster Roll, and Married To Mauve from left to right. (c) Essie nail polishes. From left to right, the colors are Tart Deco, Smokin' Hot, Mint Candy Apple, and Muchi Muchi.

We picked twelve commercially available nail polishes, representing three brands and four colors each from OPI Infinite Shine 2 long-lasting, CND Vinylux long-wear, and Essie nail

View Article Online
DOI: 10.1039/D0SM02248A

polishes (see Figure 1). Table 1 lists the typical ingredients and their concentrations. The twelve nail lacquers all rely on nitrocellulose as the film-former and have ethyl acetate and butyl acetate as active solvents. In addition to these active solvents, the so-called diluents that are poor solvents for nitrocellulose are sometimes added either as solvents for other ingredients or to help control the viscosity and drying dynamics[1]. Nitrocellulose helps in the formation of glossy, robust, and high strength coating on the nail[1, 67], primarily when used together with secondary film-formers including acrylate copolymers, di-HEMA trimethylhexyl dicarbamate, and plasticizers that reduce the glass transition temperature, T_g. Reducing T_g increases the flexibility of the nitrocellulose films, leading to improvement in wear resistance. Based on the published literature, we surmise that the nitrocellulose, typically used as film former for the nail lacquer formulations, has a nitrogen content of 10-13% and a relatively low molecular weight, M_w = 100-300 kg/mol.[78-82]

Table 1. Ingredients used in nail lacquers are listed here with their typical concentration range.

Role of the ingredient	Ingredients	Conc. (wt. %)
Film-Formers	Nitrocellulose	5-15
	Styrene/Acrylates Copolymer, Tosylamide/Formaldehyde Resin, Polyester, Tosylamide /Epoxy Resin	4-20
Plasticizers	Acetyl Tributyl Citrate, Trimethyl Pentanyl Diisobutyrate, Triphenyl Phosphate, Ethyl Tosylamide, Camphor, Trimethylpentanediyl Dibenzoate	0.1-2
Suspension Agents	Stearalkonium Bentonite, Stearalkonium Hectorite, Silica	1-5
Solvents	Ethyl Acetate, Butyl Acetate, Isopropyl Alcohol	65-75
Colorants & Pearls	Titanium Dioxide, Mica, Alumina, Synthetic Fluorphlogopite, Iron Oxides, Dyes, Calcium Aluminum Borosilicate, Aluminum Calcium Sodium Silicate, Calcium Sodium Borosilicate	0.1-10
Other additives	Benzophenone-1, Dimethicone	0.001-1

View Article Online
DOI: 10.1039/D0SM02248A

Color stabilizers, such as benzophenone-1 offset the age-dependent yellowing of the UV light-sensitive nitrocellulose. A varied proportion of pigments and colorants are added to the nail polish formulations to improve visual effects. Stable colorants, known as "lakes" (including lac lakes), are salt complexes produced by precipitated pigments from aluminum hydroxide. Certain pigments, such as mica or alumina, with a larger particle size (5 μm – 400 μm) provide sparkle or shimmer effects. In contrast, titanium oxide (and to a lesser extent iron oxide) contributes to opacity both due to high specific gravity and optical properties. Nail lacquers contain suspension agents, including organoclays added to control the flow behavior and facilitate even dispersion of colorants (especially particles). However, clays tend to aggregate into weak flocs, and their concentration, size, shape, and charge determine their influence on flow behavior, including the thixotropic response.[83-88] The formulations also contain polar additives to facilitate better clay dispersion, surfactants to improve wettability, and additional rheology modifiers, such as silica derivatives and silicones. Some additives such as vitamins, oils, herbal extracts, and proteins are sometimes added solely for marketing claims.

Methods for Characterizing Flow Behavior and Application of Nail Lacquers

We characterized the shear rheology response of nail lacquers using a cone-and-plate (cone diameter 25 mm, cone angle 1°) or a parallel plate geometry (plate diameter 25 mm, gap = 0.5 mm) using a closed-cell on an Anton Paar MCR 302 rheometer at 23 °C. Shear stress is measured for shear rates in the range $0.1-10^3$ s^{-1} and is used for determining the apparent shear viscosity, $\eta(\dot{\gamma}) = \tau/\dot{\gamma}$ for four points per decade, after applying a particular shear rate only for 10 s to minimize evaporation effects. We designed a few specialized experiments for visualizing differences between nail paints in terms of brush loading, sagging, nail coating, and dispensing/ drop formation. For these experiments, an LED white light source (Fotodiox LED-209AS) with a

View Article Online
DOI: 10.1039/D0SM02248A

color temperature set at 5600 K with a diffusor paper provides uniform illumination. The images and videos were captured using a DSLR camera (Nikon D5200 24.1 MP DSLR). The images were recorded in RAW format, and the videos were recorded at 50 fps. For carrying out the brush loading experiments, the caps, with attached brushes, were translated in an upward direction at a constant velocity of around 38 mm/s and then brought to a halt with a motorized linear stage (Velmex XSlide) using a Velmex VXM-1 stepping motor controller. We visualized subsequent dripping from the brush into the stationary bottle and compared entrainment and dripping behavior between different formulations. For the brush application experiments, the nail polish was applied to a co-author's nail by hand using similar stroke velocity for moving brush (6-10 mm/s), as human controls lead to variation. For the sagging experiments, the nail polish was poured on a piece of horizontal white paper attached to an acrylic board. Then, the board was inclined at around 60 °, and forward illumination was used for visualization.

Pinching dynamics and extensional rheology response of the nail polish formulations were characterized using the dripping-onto-substrate (DoS) rheometry protocols[36-40, 42, 43] that we developed. The experimental system used for DoS rheometry consists of a dispensing system and an imaging system. A finite volume of liquid is dispensed through a stainless-steel nozzle onto a clean glass substrate at a height H below the nozzle. The nozzle radius was kept constant for all experiments, with an outer diameter, $D_0 = 2R_0 = 2.108$ mm, and fixed values of flow rate, $Q = 0.07$ mL/min, and an aspect ratio, $H / D_0 \approx 1.5 - 3$ was used. We determined that a higher flow rate of Q = 0.07 mL/min than Q = 0.02 mL/min (typically used in our previous DoS rheometry studies) reduces the time required for creating the stretched liquid bridge. The evaporative losses are probably diminished but not eliminated (and require further investigation). The imaging system includes a light source, diffuser, and high-speed camera (Fastcam SA3). A

View Article Online
DOI: 10.1039/D0SM02248A

Nikkor 3.1 x zoom (18-25 mm) lens was used with a macro lens to maximize magnification at the frame rates used (8000 – 25000 frames per second). For the dripping-onto-substrate (DoS) experiments carried out with a DSLR camera, the images were recorded in RAM format, and the videos were recorded at 100 fps, using forward illumination. The minimum neck radius from every snapshot was determined by analyzing the DoS videos with ImageJ and specially written MATLAB codes.

RESULTS AND DISCUSSION

Shear Rheology of Twelve Nail Polishes

Figure 2 shows that the apparent shear viscosity as a function of shear rate for the twelve nail lacquer formulations exhibits shear-thinning behavior with a nearly hundred-fold decrease over a shear rate range that emulates the rates characteristic of typical processing flows.[11, 15-18, 89] A mismatch between the flow curves measured by shear rate ramp-up and the ramp-down reveals the possibility of a thixotropic response, discussed later in this section. The four-parameter Cross model[18, 90] is used for fitting the ramp-up data for the rate-dependent viscosity response for twelve formulations using the expression:

$$\eta = \eta_{\infty} + \frac{\eta_0 - \eta_{\infty}}{1 + \left(\dot{\gamma} / \dot{\gamma}_c\right)^m} \qquad (1)$$

The values of a rate-independent zero shear viscosity (η_0), high shear rate viscosity (η_{∞}), an exponent (m) that quantifies the power law dependence of the viscosity in the intermediate shear rate region, and a critical strain rate $\dot{\gamma}_c$ that defines the onset of the shear thinning region, are listed in Table 2 (in a later section). For dilute polymer solutions, parameters can be reduced to three, using solvent viscosity to define high shear rate viscosity. However, for multicomponent complex fluids like nail lacquers, the high shear rate viscosity has contributions from the

View Article Online
DOI: 10.1039/D0SM02248A

particles, polymer, and other additives, in addition to the solvent. Therefore, we used all four parameters for analysis. The zero shear viscosity and infinite shear viscosity values for a given brand appear comparable. The OPI brand nail polishes have the highest, $\eta_0 \approx (40-100\,\mathrm{Pa\cdot s})$ and nearly matched $\eta_\infty (\approx 0.4-0.6\,\mathrm{Pa\cdot s})$ values. Among the OPIs (see Figure 2a), the Big Apple Red seems to have both the highest viscosity values and the highest degree of apparent hysteresis, whereas the ramp up and down data agree for the Nessie Plays Hide & Sea-k.

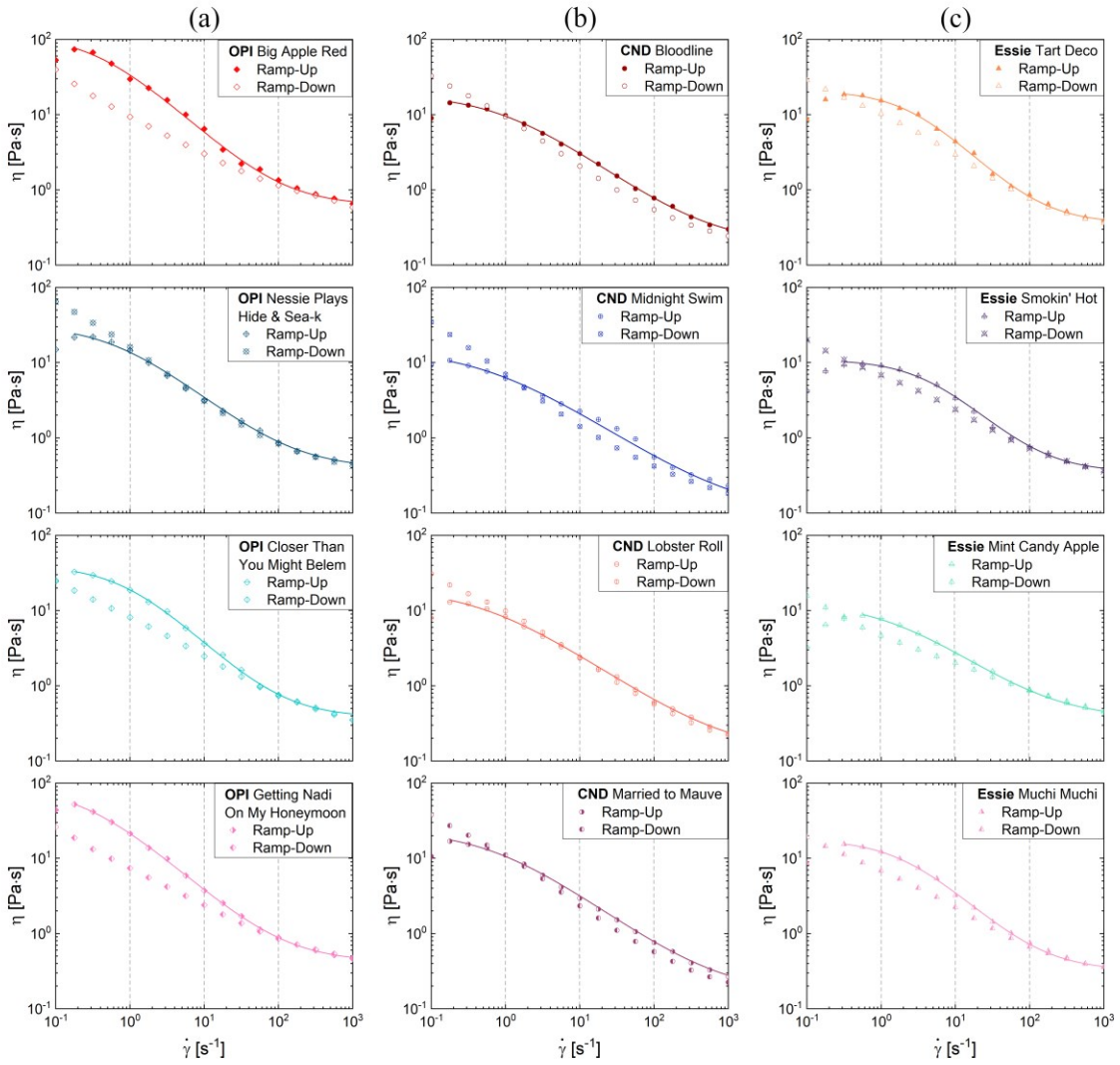

Figure 2. Apparent shear viscosity as a function of shear rate for different OPI, CND, and Essie nail polishes. A fixed time of 10 seconds is used between measured values. The difference in response to ramp-up and ramp-down attests to the different degrees of thixotropy for (a) OPI, (b) CND, and (c) Essie formulations, respectively. Cross model fits are shown as solid lines.

View Article Online
DOI: 10.1039/D0SM02248A

The two limiting viscosity values of the four CND formulations (see Figures 2b) are lower than those measured for the OPI nail polishes. The shear viscosity values are consistently lower for Essie formulations (see Figure 2c) than the OPI and CND nail lacquer formulations. Most nail polishes from the OPI brand exhibit an exponent around $m = 0.9$, whereas for the CND brand, it is typically around $m = 0.7$. We anticipate designing nail polishes with a similar degree of shear-thinning allows the use of the same manufacturing equipment, with a comparable pumping rate, aiding in the process optimization when manufacturers switch from one nail polish color or shade to another. Examination of stress *vs.* shear rate and viscosity *vs.* stress plots (see supplementary information) also show that the OPI Red exhibits a higher apparent viscosity at matched stress in contrast with the CND and Essie formulations. All nail lacquer formulations display a sharp decrease in viscosity with an increase in stress, that facilitates nail coating and dispensing processes.[12, 13] In contrast, a high value of viscosity at low shear rates improves the stability and shelf-life of suspensions and resistance to both flocculation and sedimentation.[11-13, 16, 17, 89, 91] However, for the similar reasons, bubbles trapped within the nail lacquers are long-lived,[92, 93] and users are advised to roll nail lacquer bottles, rather than shake them.[7] Bubbles and particle aggregates affect both the aesthetic and wear properties of coatings. The shape of the viscosity (or stress) *vs.* shear rate ramp-up and ramp-down data constitutes a hysteresis loop attributed to thixotropy. Like the apparent zero shear viscosity, the areas enclosed in the hysteresis loop are also smaller for the CND and Essie than the OPI formulations.

The deformation and relaxation of an underlying microstructure manifest in shear thinning and thixotropy.[83-88, 94-97] Thixotropy refers only to reversible, time-dependent, and flow-induced change in viscosity, and not all shear thinning formulations are thixotropic.[18, 56, 83-88, 95-101] Reduced particle concentration, or interactions, can lead to a lower thixotropy. Carrying out careful measurements of steady state viscosity and thixotropy response is rather challenging for

View Article Online
DOI: 10.1039/D0SM02248A

nail lacquer formulations that tend to dry quickly. However, Figure 2 presents a practical approach for characterizing thixotropic effects qualitatively in terms of the area between the ramp-up and ramp-down curves. According to Mewis and coworkers[84-88], the effect of shear rate and time can be decoupled by measuring the response to stepwise ramp in strain rate, facilitating a more rigorous characterization of thixotropic response. In Figure 3, we illustrate the measurement protocol by investigating the thixotropic response of OPI Big Apple.

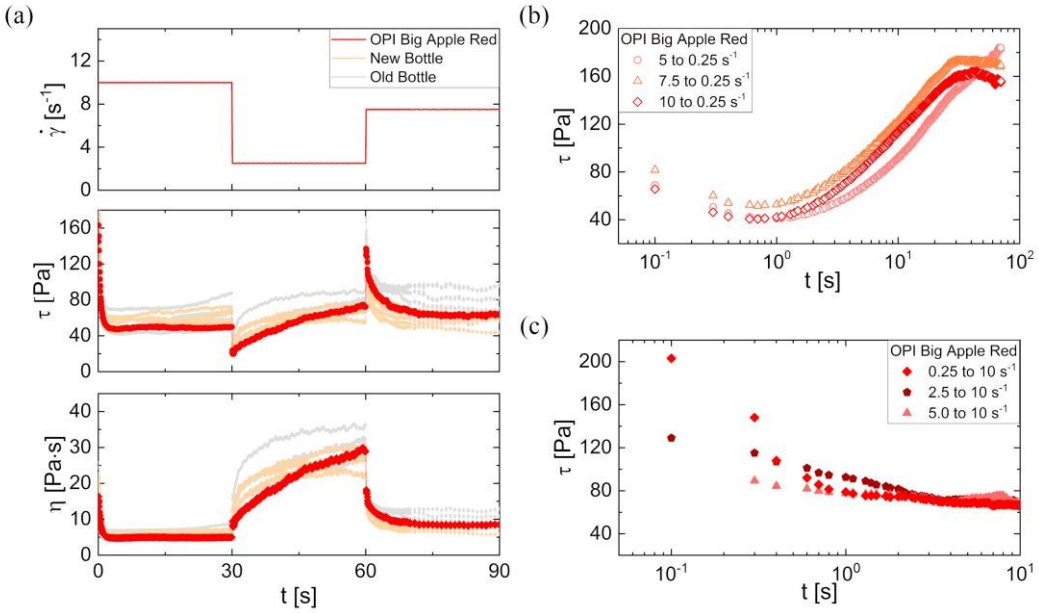

Figure 3. Time dependence response to stepwise changes in shear rate and build-up /breakdown tests for OPI shade (a) OPI Big Apple Red stress and viscosity response to different stepwise changes in shear rate starting from an initial value of 10 s^{-1}, followed by a decrease to 2.5 s^{-1} and a final value of 7.5 s^{-1}. Shear rates were imposed for a fixed time of 30 s. Multiple test results are included to highlight the characterization challenges. (b) OPI Big Apple Red stress response to a stepwise reduction in shear rates from a different initial value to a final shear rate of 0.25 s^{-1}. In all three cases, the initial shear rate was imposed until steady state values were reached. The corresponding curve with an initial shear rate of 5 s^{-1} exhibits a different and non-steady-state behavior at the longest time reported in the test. (c) OPI Big Apple Red stress response to stepwise increment in shear rates from a different initial value to a final shear rate of 10 s^{-1}. Stress values approach the same magnitude after 10 s. The initial shear rate for all three cases was applied until steady state values were reached.

Three shear rates are applied in sequence for 30 s each: an initial shear rate of 10 s^{-1} is applied, followed by a step-down to 2.5 s^{-1}, and a final step-up to 7.5 s^{-1}, as shown in Figure 3a. The measured response plotted in terms of stress and viscosity reveals that a longer time is

View Article Online
DOI: 10.1039/D0SM02248A

required to reach steady-state values on step-up in shear rate compared to the step-down processes. We include datasets from multiple experiments with the OPI Big Apple Red formulations in Figure 3a to illustrate the range of variability in these measurements (also see supplementary document for the corresponding viscosity *vs.* shear rate plots). The old bottle datasets are for samples drawn from the same bottle as used for the highlighted measurement but carried out after few months of storage. The new bottle datasets were acquired using samples drawn from a separate, freshly opened bottle. For all experiments, a pre-shear of 0.25 s^{-1} was applied for 30 s before acquiring the datasets shown here. Figure 3a appears to show a precipitous decrease in stress on step-down of shear rate typically associated with an inelastic thixotropic response. However, the stress variation plotted in Figure 3b against a log-scaled time axis shows a time-dependent decay at short times (< 1 s), that can be attributed to viscoelasticity. A thixotropic material with viscoelasticity exhibits a short, gradual decrease in stress over a timescale set by relaxation time before recovery governed by a thixotropic timescale. The datasets showing the transient response of the stress to a sudden step-down in shear rate to 0.25 s^{-1} from three distinct values of higher rates shown in Figure 3b, all show this gradual, initial decrease over 1 s and the timescale is comparable to relaxation time estimated using Cross model fit to data shown in Figure 2. The transient response for step-up to 10 s^{-1} from three lower rates is included in Figure 3c. The steady state values of the stress seem to depend weakly on the initial imposed shear rate. Due to drying problems, reversibility was not thoroughly tested by increasing shear rate back to the initial value, and a complete characterization that includes a broader range in shear rate variations was not carried out.

Brush Loading, Sagging and Leveling, and Brush Application

Nail polish is applied onto a nail typically using a miniature brush, and often, more than one layer is needed to obtain the finished look. In addition to the rheological properties of the

View Article Online
DOI: 10.1039/D0SM02248A

formulation, the mechanical and interfacial properties of the brush bristles influence the fluid volume entrained by brush on withdrawn from the bottle,[11, 102-109] the ease of forming a uniform coating, the number of coats needed, and the sensory perception of the coated films.[9, 10] Entraining, or picking up, too much product with the brush, can subsequently lead to a thicker layer and cause pooling or an uneven film. For quantitative comparison, the same brush type with different formulations, or the same formulation, with varying brush types should be used in such experiments. However, here we simply chose to use the brushes supplied with each nail polish bottle. A significant difference in entrained volume is observed as the brush mounted on a motion stage is withdrawn from the respective nail polish bottles at a controlled rate, as shown in Figure 4a (and see supplementary videos online). We observed that the considerable variation in the entrained volume contributes to the variation in the sagging and brush application process (shown in Figure 4b-c) and the subsequent dripping process (see Figure 5).

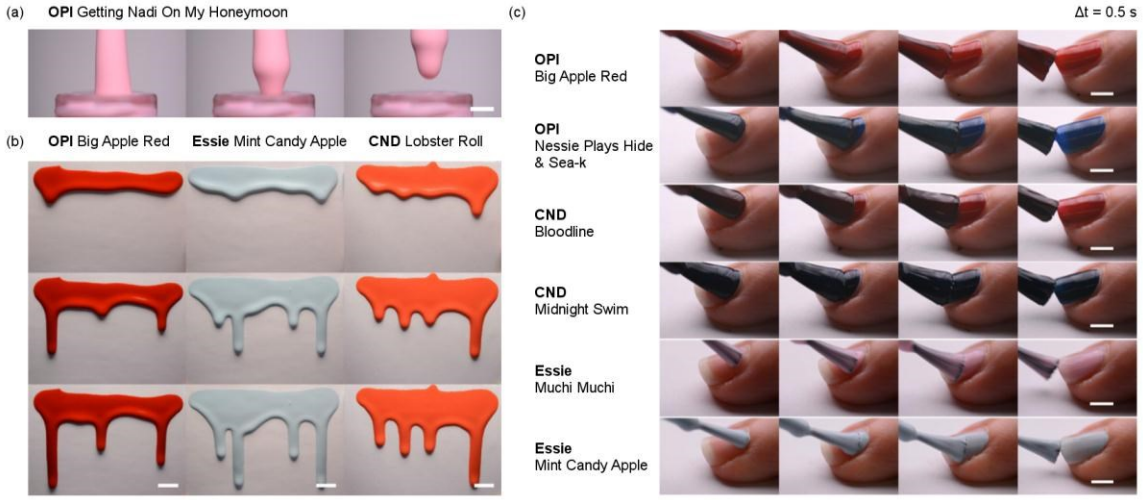

Figure 4. Visualizing volume entrained by brush loading and patterns formed during sagging. (a) The brush was mounted on a motion stage for the brush loading characterization and withdrawn at 38 mm/s. The scale bar is 3 mm. The three snapshots included are obtained using OPI Infinite Shine 2 long-lasting Getting Nadi On My Honeymoon nail polish (time step, Δt = 0.1 s). (b) Sagging of the three nail polish formulations is compared by allowing gravitational drainage of a film on a surface inclined at 60 ° (supplementary videos online). The scale bars are 10 mm each. Time difference between snapshots in each row is varied: OPI Infinite Shine 2 long-lasting nail polish with Big Apple Red color (Δt = 1.5 s), Essie nail polish with Mint Candy Apple color (Δt = 1.5 s), and CND Vinylux long-wear nail with Lobster Roll color (Δt = 0.8 s). (c) Image

View Article Online
DOI: 10.1039/D0SM02248A

sequences show nail paint application onto a fingernail using a brush moved by a human hand. The videos were acquired at 50 fps, and the scale bar is 5 mm. The brush design for CND allows for higher entrained volume. However, CND exhibits more sagging and bleeding of the formulation than OPI due to lower thixotropy and lower viscosity. Essie has a smaller brush that leads to lower pick-up or entrained volume. Also, the viscosity is lower, and the pigmentation is not as high as the other long-wear brands, such that a single brush stroke creates a more sheer finish.

Figure 4b shows representative examples of sagging as displayed by three nail polish formulations. Any commercial paint applied onto an inclined surface exhibits sagging phenomena, which refers to gravity-driven flow and finger-like pattern formation, resulting in undesirable non-uniform coats.[11-13, 110] The distance between fingers is around 27 mm for the OPI and about 17 mm for the Essie and CND formulations for the image sequences included in Figure 4b (and supplementary videos online). Sagging leads to unwanted spreading, including bleeding to the sides of a nail, requiring extra time and care for cleanup as an additional effort to beautify nails. The sagging process can be modeled as the flow of a falling film on an inclined surface by accounting for the role played by shear-thinning, and thixotropy, with the additional influence of evaporation.[110-114] Since the shear rates realized during nail coating are relatively high, control over sagging requires a faster transition to a higher viscosity fluid after removing applied stress (except gravity), and often thixotropy is considered as a possible way of reducing sagging.

In both nail paints and architectural paints, a base coat layer facilitates smoother application, protects the nail from stains, acts as a barrier between the nail polish and the nail, and assists in easier removal of the nail polish.[1, 105] Typical brush application involves an initial dipping of the brush into the polish, and after the brush withdrawal, pressing the brush to the top of the bottle helps avoid excessive dripping. We follow a similar process, and we contrast single-layer coats applied to human nails by hand. Analysis of our experiments reveals stroke speeds in the range of 5.5-10.5 mm/s, with an average velocity of 7.4 mm/s and a standard deviation error of 1.5 mm/s. The image sequences in Figure 4c show progression from right to left, with a time

View Article Online
DOI: 10.1039/D0SM02248A

step of 0.5 s, and the scale bar represents 5 mm. The stiffness of the brush can affect the film formation; stiffer bristles leave streaks behind. A proper brush should fan out on contact with the nail to provide better coverage after one stroke. However, some users prefer a smaller brush as it allows for better movement, control, and precision. We observe that the brushes for OPI and CND aided in better coverage after one stroke. Larger brush width and higher viscosity of OPI colors result in higher entrained volume than CND or Essie formulations. Lower formulation viscosity and smaller brush size limit the entrained volume, and therefore, multiple coats are necessary for obtaining a satisfying coverage. CND formulations displayed more sagging and pooling along the nail than the OPI formulations, correlated with less thixotropy as manifested in the corresponding shear rheology response. The nail polish market provides the consumer a wide range of hues and tones and a finished look that can be glossy, matte, or sheer. Though formulation rheology and the application process influence the smoothness and gloss, two rheologically-distinct formulations such as OPI Big Apple Red and CND Bloodline can provide similar color/ tone. Higher viscosity OPIs appear to have more pigmentation and exhibit a higher opacity after one brush stroke. In contrast, the Essie formulations appear to have a more sheer appearance than the other two brands.

View Article Online
DOI: 10.1039/D0SM02248A

Figure 5. Dripping is shown here for the twelve colors chosen from three different brands: OPI, CND, and Essie. Withdrawal of a brush supplied with the particular bottle was carried out at a constant velocity. Each scale bar represents 5 mm for a row of images corresponding to each brand.

Figure 5 shows snapshots of such slender jets created for each formulation after brushes are withdrawn at the same speed to a fixed height, and once enough fluid drains out, drops formed by capillarity-induced pinching can be observed. Significant contrast arises in the shape and the shape evolution of the jet as well as the pinching neck, often perceived by users as indicative of the nail lacquer formulation being too thick, thin, gooey, gloopy, or tacky. The shape evolution is influenced by capillarity, gravity, inertia, viscous stresses, and the non-Newtonian response, including extensional viscosity.[115-117] The brush entrains a larger volume of fluid for OPI Big Apple Red than for the CND Lobster Roll and Essie Mint Candy Apple. Higher entrained volume, combined with the higher viscosity of the OPI formulations and possibly the brush design, lead to a longer filament lifespan. The differences in brush design and sizes are visible in Figure 4c (and in supplementary videos online).

Pinching Dynamics of Nail Lacquer Formulations

Dispensing of cosmetic formulations typically involves a pressure-driven flow of the formulation through a nozzle, followed by free-surface flows associated with liquid transfer (by dripping or jetting) to a substrate. Streamwise velocity gradients associated with extensional flow fields arise in contracting channels, in free jets (see Figure 5) and capillarity-driven pinching of fluid necks formed during dispensing. We utilized dripping-onto-substrate (DoS) rheometry protocols (see schematic included as Figure 6i) to characterize capillarity-driven pinching dynamics of the twelve nail polishes. Unlike dripping, the DoS protocol allows for a visualization of the pinching neck at a fixed location without the influence of drop weight. The image sequences acquired with the off-the-shelf DSLR camera included in Figure 6ii display a dramatic

View Article Online
DOI: 10.1039/D0SM02248A

increase in pinching rate just before the pinch-off event. Due to the lower frame rates, fewer snapshots and data points are obtained with the DSLR camera than the high-speed camera. Therefore, we utilized a high-speed camera to visualize the pinching necks and computed radius evolution data shown in Figure 8 using our MATLAB routines. To minimize the influence of drying, we maintained a continuous flow from the nozzle between experiments and constantly cleaned the tip with ethanol. Even though the nail lacquer formulations contain nitrocellulose, the radius evolution data in Figure 8 shows no discernable viscoelastic effects, typically manifested as an elastocapillary regime with an exponential decay in radius. However, we find that we can fit the datasets for the twelve formulations by using the following expression that captures the pinching dynamics for both Newtonian and power law (Generalized Newtonian) fluids[26, 36, 38-43, 70]:

$$\frac{R(t)}{R_0} = X\left(\frac{t_f - t}{t_{xc}}\right)^{n_e} \qquad (2)$$

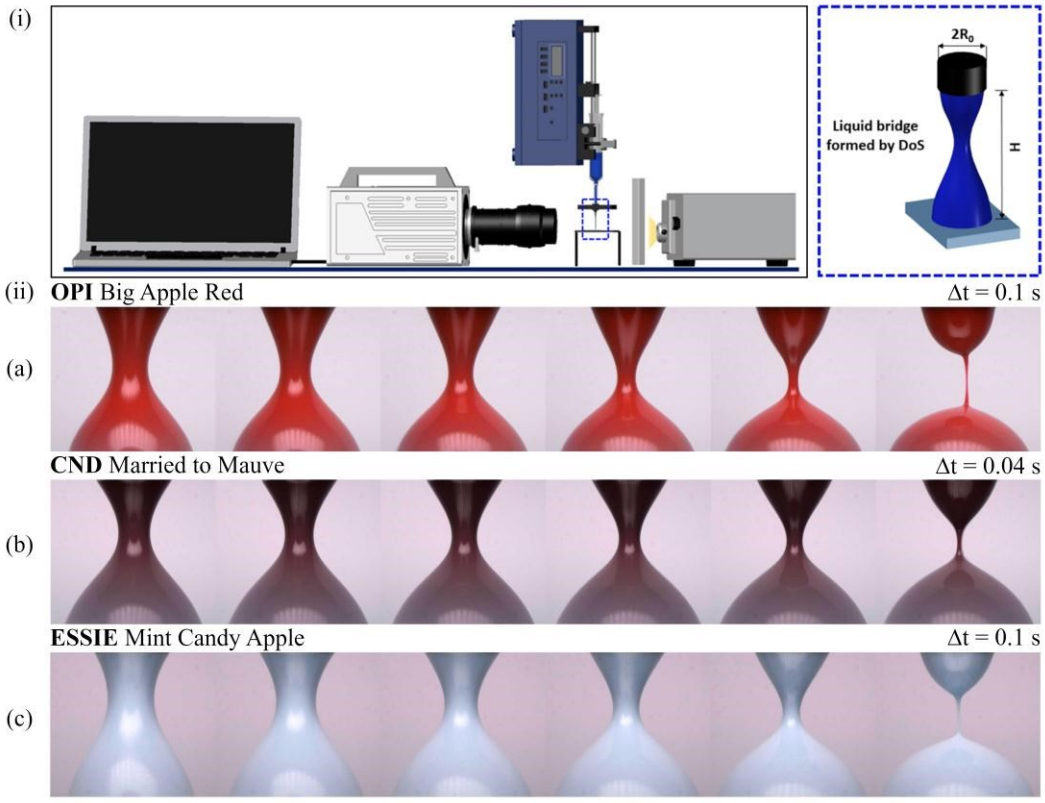

View Article Online
DOI: 10.1039/D0SM02248A

Figure 6. Schematic for Dripping-onto-Substrate (DoS) rheometry and image sequences showing shape evolution of pinching necks. (i)The set-up involves the visualization and subsequent analysis of a liquid bridge formed by a dispensing system placed between a lighting system, including a light source with a diffuser, and an imaging system including a high-speed camera and laptop. The dispensing system releases a desired amount of solution through a nozzle placed at a height *H* above a glass substrate. (ii) Image sequences acquired with a DSLR camera using 50 fps are shown for (a) OPI Big Apple Red, $\Delta t = 0.1$ s, (b) CND Married to Mauve, $\Delta t = 0.04$ s, and (c) Essie Mint Candy Apple, $\Delta t = 0.1$ s. Scale bar = 1 mm.

Low viscosity Newtonian fluids like water that exhibit inertio-capillary pinching show n_e = 0.67, neck before pinch-off event is shaped like a single cone, the characteristic timescale is inertiocapillary (IC) or Rayleigh time, $t_{xc} = t_{ic} = (\rho R_0^3/\sigma)^{1/2}$ with density, ρ, surface tension, σ, and X varies between 0.4-0.7 (as detailed elsewhere).[26, 53, 70, 118, 119] In contrast, high viscosity Newtonian fluids like glycerol that display viscocapillary regime with n_e = 1, manifest a pronounced slender, cylindrical neck, the viscocapillary time, $t_{xc} = t_{vc} = \eta R_0/\sigma$ here depends on the viscosity, η and the pre-factor X values are O(1) as detailed elsewhere.[26, 53, 70, 120, 121] Numerical results and 1-D model for shear thinning fluids[26, 39, 73-75] described by the power law model $\tau = K\dot{\gamma}^n$ with flow consistency, K and exponent, n as two parameters anticipate radius evolution with power law thinning with $n_e = n$.

View Article Online
DOI: 10.1039/D0SM02248A

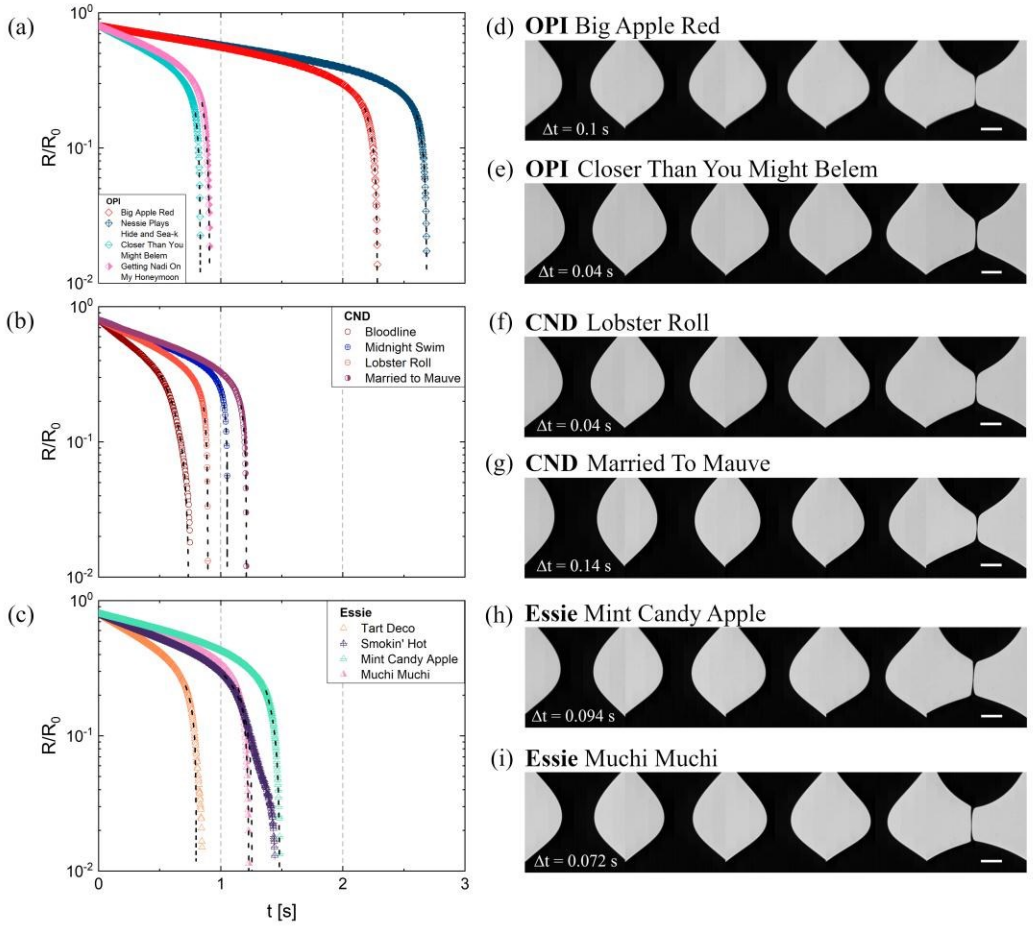

Figure 7. Radius evolution and neck shapes obtained using DoS rheometry protocols using the high-speed camera (25,000 fps) for OPI, CND, and Essie nail lacquer formulations. Radius evolution plots for the four shades of (a) OPI, (b) CND, and (c) Essie formulations. (d-e) Snapshots showing the neck shape evolution for OPI Big Apple Red, with Δt = 0.1 s, show slower change than OPI Closer Than You Might Belem with Δt = 0.04 s. (f-g) Snapshots showing the evolution of neck shape for CND Lobster Roll with Δt = 0.04 s illustrate that the pinching rate is enhanced substantially as the pinch-off event is approached compared to CND Married to Mauve shown with Δt = 0.14 s. (h-i) Essie formulations shown with Δt = 0.094 s and with Δt = 0.072 s, respectively. Scale bar = 0.5 mm.

The fits with equation 2 for the twelve formulations yield measured exponent values in the range, n_e = 0.37-0.9, as listed in Table 2 (supplementary document online shows errors on fitting parameters). Table 2 includes the four Cross model four parameters obtained by fitting the shear viscosity data shown in Figure 2. The Cross model exponent, *m,* is related to the power law exponent, *n* of the power law model $\tau = K\dot{\gamma}^n$ where K represents consistency by n = 1- m. The power law models predict $R(t)/R_0 = Y\left(t_f - t\right)^{n_e}$ with $n_e = n$ such that for $n \geq 0.6$, the

View Article Online
DOI: 10.1039/D0SM02248A

characteristic timescale, t_{PL}, depends on $Y = \Phi(n)\sigma / K = t_{PL}^{-n}$ with X=1, and the value of $\Phi(n)$ is a constant that depends on n and can be determined numerically.[26, 39, 73-75] Previous studies show that the neck shape displays two cones for $n < 0.67$, and a slender, cylindrical neck is expected for $n > 0.67$ values.[39, 73, 75] Even though radius evolution data and the image sequences included in Figure 8 reveal qualitative similarity in neck shapes and pinching dynamics between formulations explored, the formation of two cones is not observed in our experiments even for $n_e < 0.6$, and we use $t_{PL} = Y^{-1/n_e}$ to compute the characteristic timescales listed in Table 2. The comparison of λ_c and t_{PL}, the two characteristic timescales extracted from shear and extensional rheology characterization, respectively with the filament lifespan, t_f shows that the three timescales are comparable for these formulations (also see plot of λ_c and t_{PL} against t_f included in the supplementary document). We find that the exponent n_e obtained from pinching dynamics has a different value from the exponent n that describes shear thinning response. A comparison of $n = 1 - m$ and n_e data shown in Table 2, and a plot of n_e against $n = 1 - m$ included in the supplementary document, show that the two values are not correlated. Similar disagreement between n and n_e values in previous studies is attributed to the influence of deformation history on the flow behavior of highly structured complex fluids.[36, 39, 76, 97, 113, 122] Another contribution to the difference in exponents could be the role played by rate-independent viscosities measured in the limits of low (zero) and high (infinite) shear rates that are not explicitly accounted for in the simulations based on the power law model.[26, 39, 73-75]

Table 2: Shear rheology parameters for OPI, CND, and Essie nail lacquers obtained using the Cross model fits to the ramp-up flow curves are included together with the three parameters obtained by fitting a power law to the radius evolution data acquired using DoS rheometry.

Nail Lacquer Formulation	Cross Model (Torsional)				Power Law (DoS)		
	η_0 [Pa · s]	η_∞ [Pa · s]	λ_c [s]	m [-]	n_e [-]	t_f [s]	t_{PL} [s]
OPI Big Apple Red	116	0.62	2.7	0.92	0.70	2.3	1.4

View Article Online
DOI: 10.1039/D0SM02248A

OPI Nessie Plays Hide & Sea-k	32	0.39	1.6	0.83	0.61	2.7	1.3
OPI Closer Than You Might Belem	40	0.38	1.1	0.98	0.70	0.82	0.52
OPI Getting Nadi On My Honeymoon	89	0.42	3.7	0.89	0.71	0.83	0.49
CND Bloodline	19	0.19	1.0	0.74	0.62	0.64	1.1
CND Midnight Swim	15	0.10	1.5	0.66	0.38	1.0	2.3
CND Lobster Roll	20	0.13	1.8	0.70	0.54	0.90	0.85
CND Married to Mauve	24	0.16	1.5	0.74	0.54	1.1	1.0
Essie Tart Deco	21	0.36	0.40	1.0	0.51	0.81	1.5
Essie Smokin Hot	11	0.35	0.22	1.0	0.48	1.3	3.0
Essie Mint Candy Apple	13	0.37	0.69	0.76	0.75	1.5	0.93
Essie Muchi Muchi	18	0.32	0.53	0.96	0.78	1.2	0.64

The exponents and parameters obtained by analyzing pinching dynamics and the corresponding shear rheology response included in Table 2 illustrate the rich complexity in behavior observed for these multi-component formulations, even for the same product line. For example, two OPI formulations (Big Apple Red and Nessie Plays) display similar pinching behavior (comparing values of n_e and t_{PL}) shown in Figure 7a even though the zero shear viscosity values differ by a factor of 3.5. Likewise, two other OPI formulations (Closer than you Might Belem and Getting Nadi on my Honeymoon) have matched n_e and t_{PL} even though the zero shear viscosity values differ by a factor of 2. In contrast, both shear and extensional rheology response data for two Essie products (Mint Candy Apple and Essie Muchi Muchi) and two CND products (Lobster Roll and CND Married to Mauve) are fit by similar parameters. The CND Midnight Swim shows the lowest m and n_e values among all the formulations, possibly due to a relatively high amount of larger glitter particles. Several formulations, including the CND Midnight Swim, show a significant increase in thinning rate near the pinch-off event that presents

View Article Online
DOI: 10.1039/D0SM02248A

a characterization challenge, as the total number of data points obtained from snapshots is relatively low, despite a time resolution of 0.04 ms! These observations are consistent with previous studies on pinching dynamics of suspensions in Newtonian fluids that found that large particles speed up the pinching process.[123-125]

Two nail lacquer formulations (OPI Nessie Plays and CND Midnight Swim) have a shimmery appearance due to the presence of large particles, and the largest glitter particles can be observed within the pinching neck of the OPI Nessie. The radius evolution data for a couple of formulations (Essie Smokin' Hot and CND Bloodline) potentially show the existence of multiple regimes, reminiscent of studies by Mathues *et al.*,[126] among others. However, we did not pursue a detailed analysis of additional regimes as the origins of either slowing down or speeding up of pinching dynamics of particle suspensions are still under debate,[39, 123-127] and the formulations have an unspecified variation in the weight fraction and properties of innumerable ingredients. Furthermore, despite the commercial importance of the formulations like nail lacquers that contain particles dispersed in polymer solutions, the pinching dynamics and extensional rheology response of particle dispersions in viscoelastic fluids are not well-understood and well-studied using experiments or theory.[101, 128-135] Evaluating experiments carried out with the same bottle after a few days and weeks show that the pinching dynamics are sensitive to time after nail lacquers are first procured and used. Quantitative and accurate analysis of such dispersions requires proper control over the deformation history and composition of the formulations before releasing from the nozzle. Our investigations are ongoing into the influence of restructuring and relaxation times associated with particles, polymers, and aggregates or flocs formed by them and the role played by evaporative losses of volatile solvent (and the resulting change in solid fraction).

View Article Online
DOI: 10.1039/D0SM02248A

Extensional Rheology of Nail Lacquer Formulations

The apparent extensional viscosity response of the nail lacquer formulations is determined from the radius evolution data using the expression $\eta_E \dot{\varepsilon}(t) = \sigma / R(t)$ that assumes extensional and capillary stresses are the two dominant contributions to stress balance. Here the capillary stress depends on the ratio of surface tension, σ to transient neck radius, $R(t)$. The extension rate, $\dot{\varepsilon} = -2\dot{R}(t) / R(t)$ determined from the radius evolution profiles, for any values of n_e of the form captured by equation 2, always diverges close to the pinch-off event as $\dot{\varepsilon} = 2n_e/(t_f - t)$. The apparent extensional viscosity, $\eta_E = \eta_E^t(\varepsilon, \dot{\varepsilon}, t)$ can be plotted both as a function of the Hencky strain, $\varepsilon = 2\ln\left(R_0 / R(t)\right)$as shown in Figure 8a, and extensional rate, $\dot{\varepsilon}$ as shown in Figure 8b. We find that most of the nail lacquer formulations exhibit a strain-softening and extensional thinning behavior, consistent with the shear-thinning behavior exhibited in torsional rheometry measurements. The observations indicate that microstructures formed by association and clustering of pigment and suspension particles with polymers, including nitrocellulose and other additives (that are considered responsible for shear thinning behavior and thixotropy), are progressively destroyed in response to strong shear and extensional flows. However, the apparent extensional viscosity nearly approaches a strain and strain-rate independent regime for all the six formulations included in Figure 8 yielding apparent measures of steady, terminal extensional viscosity, η_E^∞ at deformation rates exceeding 10^2 s^{-1} that are listed in Table 3.

View Article Online
DOI: 10.1039/D0SM02248A

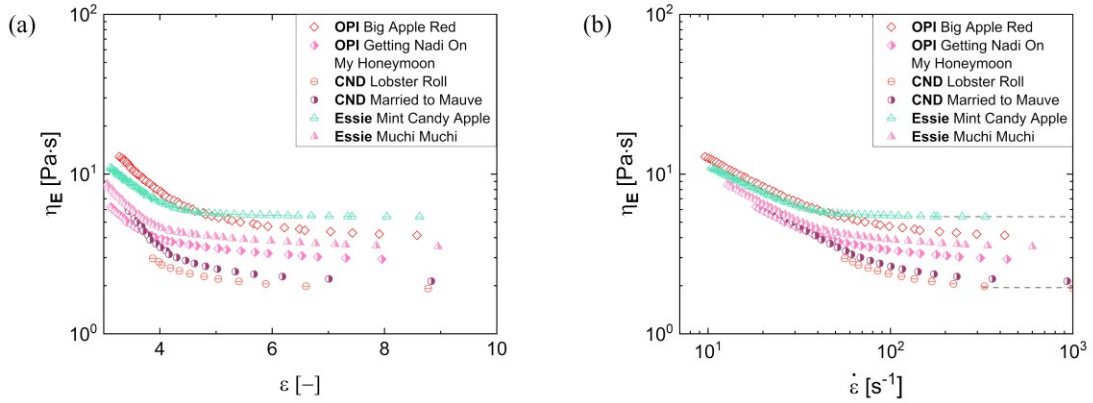

Figure 8. Contrasting variation in strain and strain rate-dependent apparent extensional viscosity. Extensional viscosity, estimated for the OPI Big Apple Red, CND Bloodline, and Essie Mint Candy Apple, is plotted as a function of (a) Hencky strain and (b) extensional rate. Extensional viscosity as a function of strain rate for all three formulations shows a nearly rate-independent plateau, though, for the OPI and Essie formulations shown, plateau arises after extensional thinning, at deformation rates exceeding 10^2 s^{-1}, whereas for after the CND Bloodline, steady values can be obtained beyond 30 s^{-1}.

The particle concentration-dependent change in shear viscosity is often discussed for particle suspensions in Newtonian fluids for both the rate-independent zero shear viscosity, η_0 and the infinite shear rate viscosity, η_∞. As nail lacquers are particle suspensions in viscoelastic fluids (polymer solution), we include both the limiting viscosity values (η_0 and η_∞) obtained from the Cross model in Table 3, and compute two estimates for Trouton ratios: η_E^∞ / η_0 and $\eta_E^\infty / \eta_\infty$, as shown in Table 3. For ultra dilute polymer solutions, shear viscosity is rate-independent and the ratio $Tr^\infty = \eta_E^\infty / \eta_0$, referred to as terminal Trouton ratio, is directly related to the square of extensibility parameter (ratio of the length of the fully stretched chain to the size of the random coil).[16, 20, 26, 36, 37, 40-43] For entangled polymer solutions that display shear thinning, $Tr \gg Tr^\infty$ implying that the ratio of extensional and shear viscosity at matched strain rate is larger, partially due to a significant decrease in shear viscosity at high shear rates.[36] Table 3 also lists η_0 / η_∞ values and we find that the zero shear viscosity values are nearly two orders of magnitude higher than the infinite shear viscosity values obtained in the limit of high deformation rates.

View Article Online
DOI: 10.1039/D0SM02248A

Table 3. Terminal Trouton ratios, defined as η_E^∞ / η_0 and $\eta_E^\infty / \eta_\infty$ obtained from ratio of the terminal extensional viscosity value (estimated from the transient extensional viscosity *vs.* extensional rate plot) and the zero shear and infinite shear viscosity, respectively (obtained from the Cross model fits to the apparent shear viscosity *vs.* shear rate data).

	η_0 [Pa · s]	η_∞ [Pa · s]	η_0 / η_∞ [-]	η_E^∞ [Pa · s]	η_E^∞ / η_0 [-]	$\eta_E^\infty / \eta_\infty$ [-]
OPI Big Apple Red	116	0.62	187	4.1	0.036	6.7
OPI Getting Nadi	89	0.42	212	2.9	0.033	7
CND Lobster Roll	20	0.13	154	1.9	0.096	15
CND Married to Mauve	24	0.16	150	2.1	0.089	13
Essie Mint Candy Apple	13	0.37	35	5.4	0.41	15
Essie Muchi Muchi	18	0.32	56	3.5	0.19	11

The *infinite* Trouton ratio, $\eta_E^\infty / \eta_\infty$ seems to be more representative of the contrasting response under processing conditions that utilize high deformation rates and yield values in the range ~6-15. The enhancement observed is consistent with the values expected based on extensional viscosity measurements reported for aqueous polysaccharide solutions and cellulose in ionic liquid, and estimates based on macromolecular extensibility.[35, 36, 41, 42, 64, 136] The values for the *infinite* Trouton ratio, $\eta_E^\infty / \eta_\infty$ in Table 3 are comparable to the high deformation rates Tr values in the range 5-16 reported by Della Valle *et al.*[137] and Ascanio *et al.*[104] for shear thinning suspensions of delaminated kaolin clays (50-65 wt.%) and coating colors (for the paper industry) prepared using carboxymethyl cellulose (CMC) thickeners, and using extensional viscosity measurements carried out with an orifice flowmeter and pressure entry technique. Likewise, O'Brien and Mackay[138] reported Trouton ratios as high as 100 and extensional thinning followed by strain hardening using orifice technique, and kaolin clay-based formulation without polymer additives but a solid fraction in a slightly higher concentration range (49-71% wt. %). Arzate *et al.*[139] observed extensional thinning with Tr < 20 for coating colors based on kaolin clay, calcium carbonate as a pigment, and CMC as a rheology modifier. The qualitative agreement in the

View Article Online
DOI: 10.1039/D0SM02248A

extensional rheology response observed for nail lacquer formulations measured using DoS rheometry and kaolin-clay based colorants used in the paper industry measured using orifice technique is rather striking, but in both cases, the formulations are optimized to meet somewhat similar demands of flow behavior during the application cycle, as summarized next.

Optimizing formulations rheology for better application and processability

Typical shear rates ($10^{-4} \leq \dot{\gamma} \leq 10^{6}\,\mathrm{s}^{-1}$) encountered during application and processing operations, including storage, sagging, and dispensing, are identified in Figure 9a, based on experiments and estimates carried out in this study and published literature.[11, 16, 17, 89, 91, 107] It is well-known that formulations, including nail lacquers, are designed to have well-defined flow properties over a very wide range of shear rates to provide relatively high viscosity and a stable dispersion at the low shear stresses usually encountered in processes related to storage. [11, 16, 17] An adequate viscosity reduction facilitates mixing and pouring and leveling and stability of the coating layer when applied to nails. Likewise, a reasonably low viscosity, but $\eta \approx O(10^{-1}\mathrm{Pa}\cdot\mathrm{s})$ is preferred at the highest rates observed during nail coating and dispensing or bottle filling[11]. Much lower viscosity (including water-like $\eta \approx O(10^{-3}\mathrm{Pa}\cdot\mathrm{s})$) makes the nail lacquer formulations appear runny, cause excessive dripping from the brush, and after application, result in undesirable sagging and spreading. Much higher viscosity, comparable to the zero shear viscosity values ($\eta > 10\,\mathrm{Pa}\cdot\mathrm{s}$) leads to an increase in perceived stringiness and tackiness, a slower rate of transfer from the brush bristle to the nail surface, and slower levelling and spreading, in addition to the need for higher stresses that can damage brush bristles. The datasets showing viscosity *vs.* shear rate obtained for the twelve formulations are included in Figure 9a. The observed rate-dependent variation in shear viscosity facilitates the processing and application of nail lacquers, including controlling entrainment, sagging, and dripping behavior (see Figure 9b). Even though formulators are well-aware of these shear rates and often vary ingredients to

View Article Online
DOI: 10.1039/D0SM02248A

obtain a desirable shear viscosity profile, typically measured for $\dot{\gamma} < 10^3\ s^{-1}$, much less attention is paid to the characterization of, and control over, pinching dynamics and extensional rheology response.

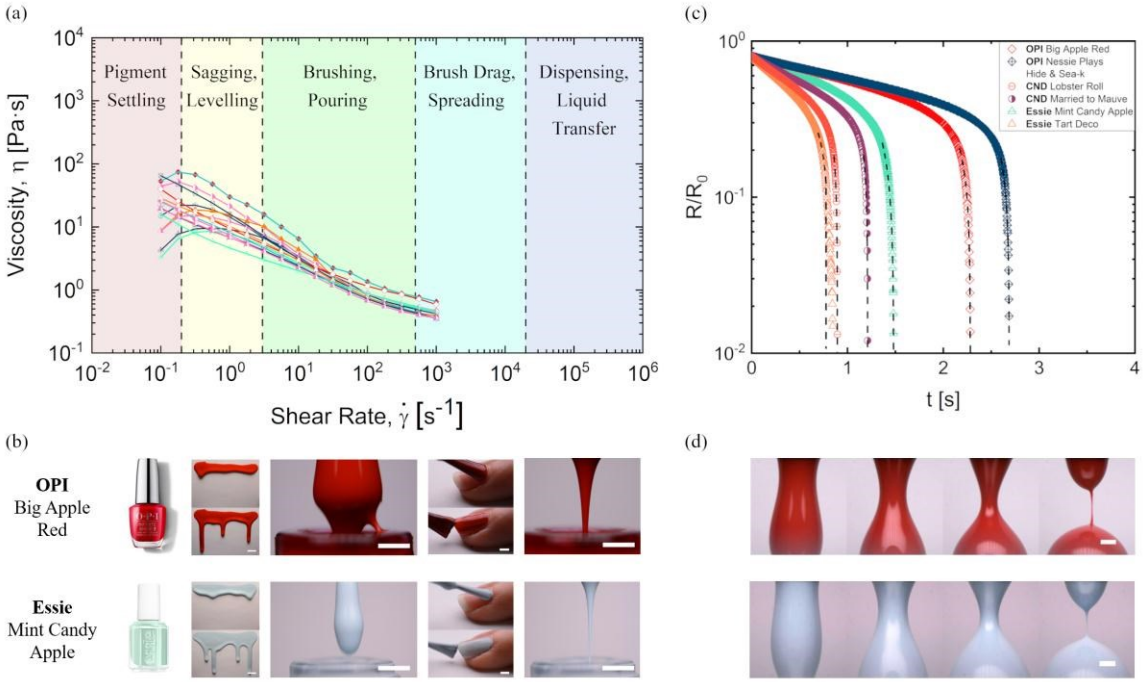

Figure 9. Optimizing rheology of nail lacquer formulations for better application and processability. (a). Shear rate ranges are associated with diverse processes that nail polishes encounter during storage, processing, and application. The plot is populated by viscosity *vs* shear rate data acquired for the OPI and Essie nail polishes. (b). Images illustrate storage, sagging, brush loading, nail polish application to a nail, and dripping for OPI Apple Red and Essie Mint Candy Apple as representative cases. The scale bars for the sagging process represent 10 mm. The scale bars for the brush loading process, brushing process, and dripping process represent 3 mm. The sagging time intervals of both nail polishes are 3 s. The brushing time intervals of OPI Infinite Shine 2 long-lasting nail polish with Big Apple Red color and Essie nail polishes with Mint Candy Apple color are 1.84 s and 1.54 s. (c) Radius evolution curves for two samples of OPI, CND, and Essie. The curves show a similar power law response at the point before pinch-off with varying pinching times t_f. (d) Image sequences for OPI Big Apple Red and Essie Mint Candy Apple acquired at 50 fps, and the scale bar represents 1 mm.

Despite the relative scarcity of datasets that capture the desirable pinching dynamics and extensional rheology response for formulations, a few qualitative expectations that be identified comprehensive survey of rheology and processing literature, discussions with formulators in coating industries, and product literature put forward by producers and consumers.[6, 7, 14, 15, 21-31] In

View Article Online
DOI: 10.1039/D0SM02248A

common parlance, consumers often talk about nail paint being too 'thick' or 'thin', and an ideal 'consistency' or 'viscosity' is needed for smoother coats and finishes. Other choice words used to describe a nail polish 'gone bad' that are indeed related to flow behavior are 'sludge-y', 'tacky', 'sticky', 'gooey', 'unspreadable', and 'lumpy'. It is well-known that over time, possibly due to the evaporative loss of the solvent, nail polish formulation can get 'thicker', or become 'gloopy' or 'goopy', often noticed on dipping a brush into the formulation, or revealed in a prolonged delay in dripping from a brush, or, sometimes, as difficulty in applying a smooth coat to nails. We qualitatively analyzed the dripping from the brush by allowing fluid entrained in the brush withdrawal experiment to fall under gravity to mimic how the consumers assess flow behavior. But variability in the number and flexibility of brush bristles, the volume of fluid entrained, and formulation rheology make comparisons difficult to untrained eyes and harder to relate to ingredient choices. We posit that the analysis of pinching dynamics included in Figure 9c-d provides a quantitative analog of the dripping from brush or stretching liquid bridges between finger and thumb experiments (and even tack tests) often used for judging stickiness, stringiness, gloopiness, or spinnability. [6, 7, 14, 15, 21-31] Here, we show radius evolution for nail lacquer formulations displays quite similar time-dependent variation captured by power laws. In addition to measurement of filament lifespan or time required for pinching, analysis of the radius evolution data allows quantitative measurement of transient extensional viscosity variation that influence the dispensing rate, coating behavior, processability where streamwise velocity gradients spontaneously arise (including converging-diverging channels and drop formation), and quite significantly, the consumer perception of fluid rheology, for arguably, humans are more sensitive to extensional rather than shear response.[14, 22-26, 140-142]

The rheological response of a nail lacquer formulation is quite similar to the overall rate-dependent shear and extensional viscosity behavior of consumer products, including food, inks,

View Article Online
DOI: 10.1039/D0SM02248A

paints and coatings, pharmaceuticals, and cosmetics that utilize polysaccharides as rheology modifiers.[19, 64, 89, 140-146] The addition of a relatively small concentration (<1% by weight) of polysaccharides like cellulose gum, guar gum, xanthan gum and nitrocellulose (added as film-formers, rheology modifiers, or thickeners) often leads to a substantial increase in zero shear viscosity and to highly shear-thinning behavior for such formulations.[22, 35, 36, 41, 64, 136, 140, 143-145] However, due to low flexibility and extensibility, the polysaccharides enhance the extensional viscosity by only an order of magnitude or so in contrast with flexible polymers that can lease to a thousand-fold enhancement for matched concentrations and molecular weights.[36, 42] The characterization of capillarity-driven pinching using CaBER, dripping, jetting, and DoS rheometry protocols have led to significant advances in understanding the influence of polymer concentration, molecular weight, and charge, and chemistry on shear and extensional viscosity of polymer solutions. A similar concerted effort that characterizes multicomponent complex fluids and connects the macroscopic response to the choice of ingredients is critically needed in designing coatings with better control on their thickness, appearance, and performance. Many challenges and research opportunities remain in the characterization of nail lacquers and similar multi-component formulations, primarily due to the difficulties associated with drying, shear thinning, thixotropy, and possible influence of viscoelastic matrix on dynamics, aggregation, and relaxation of a colloidal dispersion of pigments, suspension agents and macromolecules. We recognize that experiments with model polymers and particles will be needed to develop a deeper understanding, appropriate constitutive models, and better formulation design principles, and we anticipate the current study will inspire such studies.

CONCLUSIONS

We characterized the rheological response of twelve commercially available nail polish formulations using torsional rheometry as well as dripping-onto-substrate (DoS) rheometry. We

View Article Online
DOI: 10.1039/D0SM02248A

found that the nail lacquer formulations exhibit a pronounced degree of shear-thinning and thixotropy. The rate-dependent variation in shear viscosity was fit by the Cross model. The rate-independent zero shear viscosity is nearly two orders of magnitude larger than the limiting, infinite shear viscosity values. The Cross model exponent, *m,* that characterizes the rate-dependent decrease in shear viscosity appears to be comparable for several colors from the same product line, as matching shear thinning behavior often allows the use of similar processing equipment. We find that among the three brands selected for this study, the OPI formulations have the highest viscosity at the lowest and the highest shear rates and possess a higher degree of thixotropy. Essie formulations appear to have comparatively lower zero shear viscosity values. We devised experiments to visualize various processes associated with brush loading, nail coating, and sagging of deposited liquid films and discuss the influence of non-Newtonian rheology and fluid mechanics on these processes. The observed shear rheology response of nail lacquers is qualitatively similar to the behavior of other paints and coatings formulated using particles (used as pigments or suspending agents) and polymers (added as film formers or rheology modifiers). In all these multicomponent industrial fluids, the complex rheological response depends on, or captures, how the microstructure, formed by weakly aggregating flocs of pigments (added as colorants), clays (added as suspension agents) and polymer (added as rheology modifiers or films formers) responds to applied stress.

Unlike most published studies that explore only shear rheology response of formulations, here we carried out the analysis of pinching dynamics and extensional rheology response using the dripping-onto-substrate (DoS) rheometry protocols. The multicomponent nail lacquer formulations exemplify particle suspensions in viscoelastic solutions (that use polymer as film-former or rheology-modifier). The radius evolution data of pinching necks show a power law response with a wide range of exponent values, n_e = 0.37-0.9. Thus, like shear, the extensional

View Article Online
DOI: 10.1039/D0SM02248A

rheology response exhibits rate-thinning. Both theoretical and computational models for capillarity-driven pinching of generalized Newtonian fluids anticipate power law behavior. However, the nail lacquers exhibit a plateau value at the highest extensional rates and display power law exponents distinct from shear rheology response. Both observations are not anticipated or explained by the generalized Newtonian fluid models. We find that the strain and strain-rate independent steady, terminal extensional viscosity values are nearly an order of magnitude larger than high shear rate viscosity or infinite shear viscosity values. The infinite Trouton ratio, computed from high deformation rate extensional and shear viscosity values, is in the range of *Tr* = 7-15 and thus exhibits magnitude quite similar to the *Tr* values shown by color coatings used in the paper industry, with kaolin clay, pigments and carboxymethyl cellulose (polymer) as additives. Due to the commercial importance of particle suspensions in polymeric viscoelastic fluids, we anticipate that the protocols and datasets included in this study for diverse nail lacquer formulations will inspire the community to address the formulation and processing challenges by characterizing pinching dynamics and extensional rheology response.

Acknowledgments: CM, LNJ, and VS would like to acknowledge funding support by the PPG and the 3M nontenured faculty award. LNJ and CM were partially supported by the start-up funds as well as funded by Teaching Assistantship in the Department of Chemistry at UIC. LNJ is currently affiliated with Procter & Gamble as a postdoctoral researcher in Cincinnati, OH. CX and VS also acknowledge funding support from NSF CBET. Additionally, the authors acknowledge Dr. Samanvaya Srivastava (UCLA), Dr. Naveen Reddy (U. Hasselt), Prof. Chris Macosko (U. Minnesota), and the ODES-lab members, especially Dr. Karthika Suresh, for a close reading of the manuscript. We would like to acknowledge the discussions and insights offered by Dr. Hy Bui and Dr. Ram Hariharan (L'Oréal USA), Andrei Potanin (Colgate), Dr. Hari Katepalli (Dow), and detailed, insightful feedback from the reviewers.

View Article Online
DOI: 10.1039/D0SM02248A

REFERENCES

1. M. R. Harvey, in *Rheological Properties of Cosmetics and Toiletries*, ed. D. Laba, Routledge, 1993, pp. 153-222.
2. R. W. Sandewicz, in *Handbook of Formulating Dermal Applications*, ed. N. Dayan, John Wiley & Sons, Inc New Jersey and Scriviner Publishing, Massachussets, 2016, p. 539.
3. J. M. Barnett and R. K. Scher, *Intl. J. Dermatol.*, 1992, **31**, 675-681.
4. C. Drahl, *Chem. Eng. News*, 2008, **86**, 42.
5. C. Sun, K. Koppel and K. Adhikari, *Intl. J. Cosmetic Sci.*, 2015, **37**, 642-650.
6. C. Sun, K. Koppel and E. Chambers, *Intl. J. Cosmetic Sci.,* 2014, **36**, 262-272.
7. Hellomagazine.com, How to solve common nail problems, https://www.hellomagazine.com/healthandbeauty/2015080726603/nailproblem-how-to-solve-them/, (accessed 12/18/2020, 2020).
8. P. Walter and L. de Viguerie, *Nat. Mater.*, 2018, **17**, 106.
9. K. J. Mysels, *Leonardo*, 1981, 22-27.
10. G. W. S. Blair, *Leonardo*, 1969, 51-53.
11. R. Lambourne and T. A. Striven, eds., *Paint and Surface Coatings: Theory and Practice*, Woodhead Publishing Ltd, Cambridge, U. K., 1999.
12. R. R. Eley, *J. Coatings Tech. Res.*, 2019, **16**, 263-305.
13. R. R. Eley, *Rheology Rev.*, 2005, 173-240.
14. Z. Lv, J. Chen and M. Holmes, *J. Texture Stud.*, 2017, **48**, 463-469.
15. L. N. Jimenez, C. D. V. M. Narváez, C. Xu, S. Bacchi and V. Sharma, *Surface Science and Adhesion in Cosmetics*, 2021, 109-150.
16. R. G. Larson, *The Structure and Rheology of Complex Fluids*, Oxford University Press, New York, 1999.
17. C. W. Macosko, *Rheology: Principles, Measurements and Applications*, VCH Publishers Inc, New York, 1994.
18. H. A. Barnes, J. F. Hutton and K. Walters, *An Introduction to Rheology*, Elsevier Science Publishers B. V., Amsterdam, 1989.
19. P. Fischer and E. J. Windhab, *Curr. Opin. Colloid Interface Sci.*, 2011, **16**, 36-40.
20. T. Q. Nguyen and H. H. Kausch, *Flexible Polymer Chains in Elongational Flow: Theory and Experiment*, Springer-Verlag, Berlin, 1999.
21. C. J. S. Petrie, *J. Non-Newtonian Fluid Mech.*, 2006, **137**, 1-14.
22. L. Gilbert, V. Loisel, G. Savary, M. Grisel and C. Picard, *Carbohydr. Polym.*, 2013, **93**, 644-650.
23. L. Gilbert, C. Picard, G. Savary and M. Grisel, *J. Sens. Stud.*, 2012, **27**, 392-402.
24. A. Ahuja and A. Potanin, *Rheol. Acta*, 2018, **57**, 459-471.
25. A. Ahuja, J. Lu and A. Potanin, *J. Texture Stud.*, 2019, **50**, 295-305.
26. G. H. McKinley, *Rheology Rev.*, 2005, 1-48.
27. C. Creton and M. Ciccotti, *Rep. Prog. Phys.*, 2016, **79**, 046601.
28. C. Verdier and J. M. Piau, *J. Polym. Sci., Part B: Polym. Phys.*, 2003, **41**, 3139-3149.
29. B. Adhikari, T. Howes, B. R. Bhandari and V. Truong, *Intl. J. Food Prop.*, 2001, **4**, 1-33.
30. A. Tai, R. Bianchini and J. Jachowicz, *Intl. J. Cosmetic Sci.*, 2014, **36**, 291-304.
31. L. S. Calixto and P. M. B. G. Maia Campos, *Intl. J. Cosmetic Sci.*, 2017, **39**, 527-534.
32. M. D. Graham, *Phys. Fluids*, 2003, **15**, 1702.

View Article Online
DOI: 10.1039/D0SM02248A

33. L. E. Rodd, T. P. Scott, J. J. Cooper-White and G. H. McKinley, *Appl. Rheol.*, 2005, **15**, 12-27.
34. D. F. James and K. Walters, in *Techniques of Rheological Measurement*, ed. A. A. Collyer, Elsevier, New York, 1994, ch. 2, pp. 33-53.
35. V. Sharma, S. J. Haward, J. Serdy, B. Keshavarz, A. Soderlund, P. Threlfall-Holmes and G. H. McKinley, *Soft Matter*, 2015, **11**, 3251-3270.
36. J. Dinic and V. Sharma, *Macromolecules*, 2020, **53**, 3424-3437.
37. J. Dinic, Y. Zhang, L. N. Jimenez and V. Sharma, *ACS Macro Lett.*, 2015, **4**, 804-808.
38. J. Dinic, M. Biagioli and V. Sharma, *J. Polym. Sci., Part B: Polym. Phys.*, 2017, **55**, 1692-1704.
39. J. Dinic, L. N. Jimenez and V. Sharma, *Lab Chip*, 2017, **17**, 460-473.
40. L. N. Jimenez, J. Dinic, N. Parsi and V. Sharma, *Macromolecules*, 2018, **51**, 5191-5208.
41. L. N. Jimenez, C. D. V. Martínez Narváez and V. Sharma, *Phys. Fluids*, 2020, **32**, 012113.
42. J. Dinic and V. Sharma, *Macromolecules*, 2020, **53**, 4821-4835.
43. J. Dinic and V. Sharma, *Proc. Natl. Acad. Sci. U.S.A.*, 2019, **116**, 8766–8774.
44. K. W. Hsiao, J. Dinic, Y. Ren, V. Sharma and C. M. Schroeder, *Phys. Fluids*, 2017, **29**, 121603.
45. A. V. Walter, L. N. Jimenez, J. Dinic, V. Sharma and K. A. Erk, *Rheol. Acta*, 2019, **58**, 145-157.
46. K. A. Marshall, A. M. Liedtke, A. H. Todt and T. W. Walker, *Exp. Fluids*, 2017, **58:69**, 9.
47. N. S. Suteria, S. Gupta, R. Potineni, S. K. Baier and S. A. Vanapalli, *Rheol. Acta*, 2019, **58**, 403-417.
48. K. A. Marshall and T. W. Walker, *Rheol. Acta*, 2019, **58**, 573-590.
49. M. Rosello, S. Sur, B. Barbet and J. P. Rothstein, *J. Non-Newtonian Fluid Mech.*, 2019, **266**, 160-170.
50. Y. Zhang and S. J. Muller, *Phys. Rev. Fluids*, 2018, **3**.
51. S. J. Wu and H. Mohammadigoushki, *J. Rheol.*, 2018, **62**, 1061-1069.
52. R. Omidvar, S. Wu and H. Mohammadigoushki, *J. Rheol.*, 2019, **63**, 33-44.
53. J. Dinic and V. Sharma, *Phys. Fluids*, 2019, **31**, 021211.
54. J. Jefferson and P. Rich, *Dermatologic Therapy*, 2012, **25**, 481-490.
55. F. Brunello, *The Art of Dyeing in the History of Mankind*, Neri Pozza, New York, 1973.
56. S. V. Berbers, D. Tamburini, M. R. van Bommel and J. Dyer, *Dyes and Pigments*, 2019, **170**, 107579.
57. J. Dyer, D. Tamburini and S. Sotiropoulou, *Dyes Pigm.*, 2018, **149**, 122-132.
58. R. Castro, A. Miranda and M. J. Melo, *Sources on Art Technology: Back to Basics. London: Archetype Publications*, 2016, 88-99.
59. C. S. Smith and J. G. Hawthorne, *Trans. Am. Philos. Soc.*, 1974, **64**, 1-128.
60. P. C. Ray, *A History of Hindu Chemistry from the Earliest Times to the Middle of the Sixteenth Century, AD: With Sanskrit Texts, Variants, Translation and Illustrations*, Williams and Norgate, 1909.
61. D. N. Carvalho, *Forty Centuries of Ink*, Banks Law Publishing Co., New York, 1904.
62. L. de Viguerie, G. Ducouret, F. Lequeux, T. Moutard-Martin and P. Walter, *C R Phys.*, 2009, **10**, 612-621.
63. M. P. Aguilar, M. J. H. Lucas and M. D. Planas, in *Science and Technology for the Conservation of Cultural Heritage*, CRC Press, 2013, pp. 221-224.
64. C. Clasen and W. M. Kulicke, *Prog. Polym. Sci.*, 2001, **26**, 1839-1919.

View Article Online
DOI: 10.1039/D0SM02248A

65. R. Zenit, *Phys. Rev. Fluids*, 2019, **4**, 110507.
66. E. C. Worden, *Nitrocellulose Industry*, D. Van Nostrad Co., New York, , 1911.
67. R. B. Seymour and G. B. Kauffman, *J. Chem. Educ.*, 1992, **69**, 311.
68. E. Theisen, *J. Soc. Motion Pict. Eng.*, 1933, **20**, 259-262.
69. M. Iqbal, J. Y. S. Li-Mayer, D. Lewis, S. Connors and M. N. Charalambides, *Phys. Fluids*, 2020, **32**, 023103.
70. J. Eggers, *Rev. Mod. Phys.*, 1997, **69**, 865-929.
71. J. Eggers and M. A. Fontelos, *Singularities: Formation, Structure, and Propagation*, Cambridge University Press, Cambridge, UK, 2015.
72. O. A. Basaran, *AIChE J.*, 2002, **48**, 1842-1848.
73. P. Doshi, R. Suryo, O. E. Yildirim, G. H. McKinley and O. A. Basaran, *J. Non-Newtonian Fluid Mech.*, 2003, **113**, 1-27.
74. P. Doshi and O. A. Basaran, *Phys. Fluids*, 2004, **16**, 585-593.
75. R. Suryo and O. A. Basaran, *J. Non-Newtonian Fluid Mech.*, 2006, **138**, 134-160.
76. F. M. Huisman, S. R. Friedman and P. Taborek, *Soft Matter*, 2012, **8**, 6767-6774.
77. K. Niedzwiedz, H. Buggisch and N. Willenbacher, *Rheol. Acta*, 2010, **49**, 1103-1116.
78. S. T. Kim, J. Y. Lim, H. J. Choi and H. Hyun, *J. Ind. Eng. Chem.*, 2006, **12**, 161-164.
79. C. H. Lindsley and M. B. Frank, *Ind. Eng. Chem.*, 1953, **45**, 2491-2497.
80. W. Koch, H. C. Phillips and R. Wint, *Ind. Eng. Chem.*, 1945, **37**, 82-86.
81. W. Koch, H. C. Phillips and R. Wint, *Ind. Eng. Chem.*, 1946, **38**, 518-521.
82. H. E. Hofmann and E. W. Reid, *Ind. Eng. Chem.*, 1928, **20**, 687-694.
83. H. A. Barnes, *J. Non-Newtonian Fluid Mech.*, 1997, **70**, 1-33.
84. K. Dullaert and J. Mewis, *J. Rheol.*, 2005, **49**, 1213-1230.
85. K. Dullaert and J. Mewis, *J. Non-Newtonian Fluid Mech.*, 2006, **139**, 21-30.
86. J. Mewis and N. J. Wagner, *Adv. Colloid Interface Sci.*, 2009, **147**, 214-227.
87. P. C. F. Møller, J. Mewis and D. Bonn, *Soft Matter*, 2006, **2**, 274-283.
88. J. Mewis and N. J. Wagner, *Colloidal Suspension Rheology*, Cambridge University Press, 2011.
89. R. Lapasin and S. Pricl, *Rheology of Industrial Polysaccharides: Theory and Applications*, Chapman & Hall, London, 1995.
90. M. M. Cross, *J. Colloid Sci.*, 1965, **20**, 417-437.
91. S. Paul, *Surface Coatings: Science and Technology*, John Wiley & Sons, New York, 1985.
92. D. C. Venerus, *J. Non-Newtonian Fluid Mech.*, 2015, **215**, 53-59.
93. W. F. Lopez, M. F. Naccache and P. R. de Souza Mendes, *J. Rheol.*, 2018, **62**, 209-219.
94. M. Dinkgreve, J. Paredes, M. M. Denn and D. Bonn, *J. Non-Newtonian Fluid Mech.*, 2016, **238**, 233-241.
95. D. Bonn, M. M. Denn, L. Berthier, T. Divoux and S. Manneville, *Rev. Mod. Phys.*, 2017, **89**, 035005.
96. A. Z. Nelson, R. E. Bras, J. Liu and R. H. Ewoldt, *J. Rheol.*, 2018, **62**, 357-369.
97. P. Coussot, *J. Non-Newtonian Fluid Mech.*, 2014, **211**, 31-49.
98. D. C.-H. Cheng, *Intl. J. Cosmetic Sci.*, 1987, **9**, 151.
99. Y. M. Joshi, *Annu. Rev. Chem. Biomol. Eng*, 2014, **5**, 181-202.
100. P. R. de Souza Mendes and R. L. Thompson, *Curr. Opin. Colloid Interface Sci.*, 2019, **43**, 15-25.
101. H. A. Barnes, *Rheology Reviews*, 2003, 1-36.
102. D. Quere, *Ann. Rev. Fluid. Mech.*, 1999, **31**, 347-384.

View Article Online
DOI: 10.1039/D0SM02248A

103. B. Scheid, J. Delacotte, B. Dollet, E. Rio, F. Restagno, E. A. van Nierop, I. Cantat, D. Langevin and H. A. Stone, *EPL*, 2010, **90**.
104. G. Ascanio, P. J. Carreau and P. A. Tanguy, *Exp. Fluids*, 2006, **40**, 1-14.
105. J. E. Glass and R. K. Prud'homme, in *Liquid Film Coating*, Springer, 1997, pp. 137-182.
106. J. S. Ro and G. M. Homsy, *J. Non-Newtonian Fluid Mech.*, 1995, **57**, 203-225.
107. K. J. Ruschak, *Ann. Rev. Fluid. Mech.*, 1985, **17**, 65-89.
108. S. J. Weinstein and K. J. Ruschak, *Annu. Rev. Fluid Mech.*, 2004, **36**, 29-53.
109. G. Zevallos, M. Carvalho and M. Pasquali, *J. Non-Newtonian Fluid Mech.*, 2005, **130**, 96-109.
110. D. R. Hewitt and N. J. Balmforth, *J. Fluid Mech.*, 2013, **727**, 56-82.
111. H. T. Huynh, N. Roussel and P. Coussot, *Phys. Fluids*, 2005, **17**, 033101.
112. A. Oron, S. H. Davis and S. G. Bankoff, *Rev. Mod. Phys.*, 1997, **69**, 931.
113. P. Coussot and F. Gaulard, *Phys. Rev. E.*, 2005, **72**, 031409.
114. L. Espín and S. Kumar, *Langmuir*, 2014, **30**, 11966-11974.
115. J. Château and H. Lhuissier, *Phys. Rev. Fluids*, 2019, **4**, 012001.
116. J. Château, É. Guazzelli and H. Lhuissier, *J. Fluid Mech.*, 2018, **852**, 178-198.
117. S. Middleman, *Modeling Axisymmetric Flows: Dynamics of Films, Jets and Drops*, Academic Press, San Diego, 1995.
118. Y.-J. Chen and P. H. Steen, *J. Fluid Mech.*, 1997, **341**, 245-267.
119. R. F. Day, E. J. Hinch and J. R. Lister, *Phys. Rev. Lett.*, 1998, **80**, 704-707.
120. G. H. McKinley and A. Tripathi, *J. Rheol.*, 2000, **44**, 653-670.
121. J. R. Castrejón-Pita, A. A. Castrejón-Pita, S. S. Thete, K. Sambath, I. M. Hutchings, J. Hinch, J. R. Lister and O. A. Basaran, *Proc. Natl. Acad. Sci. U.S.A.*, 2015, **112**, 4582-4587.
122. N. Louvet, D. Bonn and H. Kellay, *Phys. Rev. Lett.*, 2014, **113**, 218302.
123. C. Bonnoit, T. Bertrand, E. Clément and A. Lindner, *Phys. Fluids*, 2012, **24**, 043304.
124. M. S. van Deen, T. Bertrand, N. Vu, D. Quéré, E. Clément and A. Lindner, *Rheol. Acta*, 2013, **52**, 403-412.
125. R. J. Furbank and J. F. Morris, *Phys. Fluids*, 2004, **16**, 1777-1790.
126. W. Mathues, C. McIlroy, O. G. Harlen and C. Clasen, *Phys. Fluids*, 2015, **27**, 093301.
127. M. I. Smith, R. Besseling, M. E. Cates and V. Bertola, *Nature Comm.*, 2010, **1**, 1-5.
128. E. S. G. Shaqfeh, *AlChE J.*, 2019, **65**, e16575.
129. S. Khandavalli and J. P. Rothstein, *J. Rheol.*, 2014, **58**, 411-431.
130. F. Greco, G. D'Avino and P. L. Maffettone, *J. Non-Newtonian Fluid Mech.*, 2007, **147**, 1-10.
131. N. A. Patankar and H. H. Hu, *J. Non-Newtonian Fluid Mech.*, 2001, **96**, 427-443.
132. D. L. Koch and G. Subramanian, *J. Non-Newtonian Fluid Mech.*, 2006, **138**, 87-97.
133. S.-C. Dai, F. Qi and R. I. Tanner, *J. Rheol.*, 2014, **58**, 183-198.
134. J. Einarsson, M. Yang and E. S. Shaqfeh, *Phys. Rev. Fluids*, 2018, **3**, 013301.
135. A. Jain, J. Einarsson and E. S. G. Shaqfeh, *Phys. Rev. Fluids*, 2019, **4**, 091301.
136. S. J. Haward, V. Sharma, C. P. Butts, G. H. McKinley and S. S. Rahatekar, *Biomacromolecules*, 2012, **13**, 1688-1699.
137. D. Della Valle, P. A. Tanguy and P. J. Carreau, *J. Non-Newtonian Fluid Mech.*, 2000, **94**, 1-13.
138. V. T. O'brien and M. E. Mackay, *J. Rheol.*, 2002, **46**, 557-572.
139. A. Arzate, G. Ascanio, P. J. Carreau and P. A. Tanguy, *Appl. Rheol.*, 2004, **14**, 240-250.

View Article Online
DOI: 10.1039/D0SM02248A

140. A. Theocharidou, M. Ahmad, D. Petridis, C. Vasiliadou, J. Chen and C. Ritzoulis, *Food Hydrocoll.*, 2021, **111**, 106246.
141. L. Zhong, E. K. Hadde, Z. Zhou, Y. Xia and J. Chen, *J. Sens. Stud.*, 2018, **33**, e12464.
142. Q. He, J. Hort and B. Wolf, *Food Hydrocoll.*, 2016, **61**, 221-232.
143. T. Wüstenberg, *Cellulose and Cellulose Derivatives in the Food Industry: Fundamentals and Applications*, John Wiley & Sons, 2014.
144. S. Dumitriu, ed., *Polysaccharides: Structural Diversity and Functional Versality*, Marcel Dekker, New York, 2005.
145. S. Morozova, P. W. Schmidt, A. Metaxas, F. S. Bates, T. P. Lodge and C. S. Dutcher, *ACS MacroLetters*, 2018, **7**, 347-352.
146. G. Savary, M. Grisel and C. Picard, in *Natural Polymers: Industry Techniques and Applications*, ed. O. Olatunji, Springer, 2016, pp. 219-261.